

Electrodeposition of Cu₂O thin Film Onto Copper Substrate by Linear Sweep Voltammetry at Low Duration: Effect of Bath pH

Khalid Jrajri ¹, Mustapha Beraich ^{1,2,*} , Ismail Warad ³, Abdallah Guenbour ¹, Abdelkadir Bellaouchou ¹, Abdelkader Zarrouk ¹

¹ Laboratory of Materials, Nanotechnology, and Environment, Faculty of Sciences, Mohammed V University, P.O. Box. 1014 Agdal-Rabat, Morocco

² Laboratory of Physics Materials and Subatomic (LPMS), Department of Physics, Ibn Tofail University, Kenitra, Morocco

³ Department of Chemistry and Earth Sciences, P.O. Box 2713, Qatar University, Doha, Qatar

* Correspondence: beraichagr@gmail.com (B.M);

Scopus Author ID 36125763200

Received: 23.09.2021; Revised: 1.11.2021; Accepted: 4.11.2021; Published: 28.11.2021

Abstract: Copper (II) oxide (Cu₂O) has attracted much interest as a semiconductor material for solar cell applications. Here we report the synthesis of Cu₂O, thin films through an economical and simple electrodeposition method at low duration (10 min) by linear sweep voltammetry (LSV) method at 50 °C bath temperature, with the use of citric acid as a complexing agent. The influence of pH value (pH = 9.5, 10.5, 11.5, and 12.5) on structural, morphological, and optical properties of the synthesized Cu₂O thin films onto copper substrate was investigated. The synthesized Cu₂O thin films have been characterized using various techniques like X-ray diffraction (XRD), Raman spectroscopy, Scanning Electron Microscopy (SEM-EDX), UV-vis spectrophotometry. The X-ray diffraction showed that the deposited thin films at pH= 9.5, 10.5, 11.5 matched well with the cubic (Pn-3m) structure and showed an improvement of the crystallinity near the value pH=10.5. Raman spectroscopy confirms the cubic structure of the synthesized thin film. Thin films show a high absorption coefficient in the visible spectra, and the calculated band gap energy value is near 1.8 eV.

Keywords: Cu₂O; electrodeposition; linear voltammetry; thin films, bandgap; solar cells.

© 2021 by the authors. This article is an open-access article distributed under the terms and conditions of the Creative Commons Attribution (CC BY) license (<https://creativecommons.org/licenses/by/4.0/>).

1. Introduction

Solar energy is the most abundant energy on earth. In fact, the earth receives in one day the equivalent of energy that can cover the consumption of one year. Photovoltaic cells are the more appropriate choice for converting solar energy into electricity. This has led to thin-film solar cell technology developments due to their flexibility, low weight, low consumption of raw materials, and low-cost manufacturing [1-3].

The metal oxide material has been found interesting for use as absorbing layers in solar cells, especially the copper (II) oxide Cu₂O, due to its suitable bandgap ($E_g=1.8-2.2$ eV), high absorption coefficient ($\approx 10^5$ cm⁻¹) in the visible- near-infrared spectra, earth-abundance and the non-toxicity of copper element [4-7].

In addition to its application in solar cells, this material offers great freedom. It can be used in different applications and thus satisfies industrial demands [8]. Among these remarkable applications, we find the use of Cu₂O material in photocatalytic material [9-11], photoelectrochemical cell [12-14], photodetector [15], thermoelectric [16], photodiode devices

[17], and electrochromic material [18]. Also, Cu₂O was introduced as an attractive anode material for sodium-ion battery systems [19]. Therefore, the investigation of this material as absorber material in solar cells was the goal of this study.

The low-cost production of thin-film solar cells has become the first preoccupation of the optoelectronic industry. The Cu₂O thin film can be synthesized using several physical and chemical methods such as chemical deposition technique [20], spray deposition [21], electrodeposition [22-26], chemical bath deposition [27], thermal evaporation [28], spin coating [29], vacuum diffusion [30], and SILAR [31].

Electrodeposition technic is a simple and low-cost technic, is a successful method for the deposition of quaternary, ternary, and binary material like Cu₂-II-Sn-S₄, Cu₂-Sn-S₃, and Cu₂O [32-35]. The electrodeposition method allows for controlling the physical, optical, and electrical characteristics of thin films by varying several factors such as the thickness of the film, bath composition, concentration, time of electrodeposition, the temperature of bath, pH, and potential of electrodeposition.

The pH is an important parameter for the synthesis of thin film by electrodeposition. For this reason, in the present work, the Cu₂O thin films were synthesized by electrodeposition method onto the copper substrate, using citric acid as a complexing agent. Also, the influence of pH on structural, morphological, and optical properties of the synthesized Cu₂O thin films was investigated using X-ray diffraction (XRD), energy dispersive spectroscopy (EDX), Raman spectroscopy, and UV-Visible – NIR spectrophotometry.

2. Materials and Methods

The Cu₂O thin films were deposited onto copper substrates using the electrodeposition method. Before Cu₂O thin films deposition, four equimolar solutions of Cu²⁺ and citric acid (0.05 M) were prepared by dissolution the appropriate mass of copper sulfate (CuSO₄, Sigma -Aldrich, 99%) citric acid. (C₆H₈O₇, Sigma -Aldrich, 99.8%) in 25ml of distilled water, the pH of the four solutions was adjusted to 9.5, 10.5, 11.5, and 12.5, respectively, using sodium hydroxide. The citric acid was used as a complexing agent to increase the solubility of Cu²⁺ ions and avoid their precipitation in basic media.

The Cu-substrates were ultrasonically cleaned for 15 min sequentially in dilute hydrochloric acid, acetone, ethanol, distilled water and then dried in the air before being used for deposition. The Cu₂O thin films were synthesized by linear sweep voltammetry (LSV) method by the use of the three mounting electrodes connected to the potentiostat-galvanostat Origa-Flex. The potential was varied between -0.2V and -0.4V/SCE, and the scan rate was fixed at 0.3 mV/s.

Finally, the samples were then taken out and washed with distilled water, and dried in air at ambient temperature. The obtained films were characterized by an XPERT-3 X-ray diffractometer with a copper source monochromatic Cu-K α_1 radiation $\lambda = 1.5406 \text{ \AA}$. The determination of surface morphology and composition of the deposited thin films were obtained by scanning electron microscopy (SEM) equipped with energy-dispersive X-ray spectroscopy (EDX) and also with an element mapping scan. For optical properties, the JASCO V-670 spectrophotometer was used to measure the absorbance spectra with a wavelength range of 190 to 2700 nm. The Raman spectroscopy measurement was conducted using a Bruker RAM (II) FT-Raman spectrometer in the range of 100 to 700 cm⁻¹.

3. Results and Discussion

3.1. Structural characterization.

Figure 1 displays the XRD spectra of all deposited Cu₂O thin films with different pH values (9.5, 10.5, 11.5, and 12.5). The peak at 2θ = 36.42° corresponds to the (111) plane of Cu₂O in cubic structure ((Pn-3m space group), which is in good agreement with the standard Data card (JCPDS # 00-005-0667) and with other reports [36]. The (111) diffraction peaks become more pronounced for the synthesized Cu₂O thin film at pH=10.5. In addition, all the synthesized Cu₂O thin films show a preferential orientation of the crystallites along the (111) direction due to the influence of copper substrate [36]. The XRD shows that the pH=12.5 did not allow the formation of the Cu₂O thin film. Therefore, in the next section, we will only discuss the Cu₂O layers successfully formed at 9.5, 10.5, and 11.5.

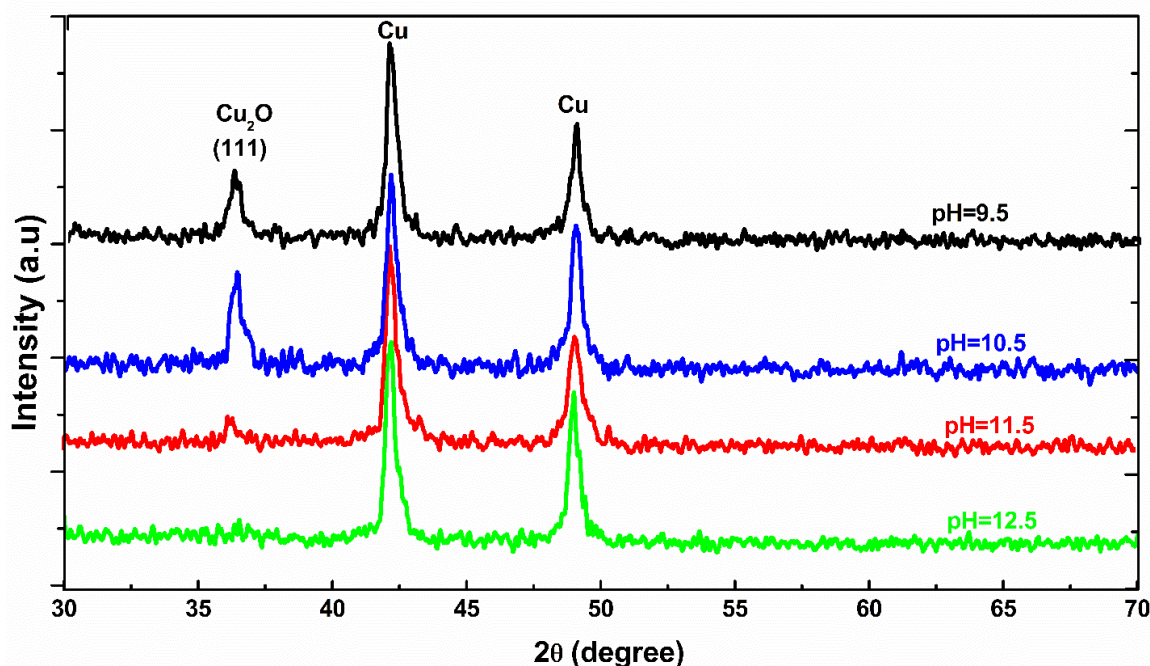


Figure 1. XRD patterns of Cu₂O thin films electrodeposited with various pH bath values (9.5, 10.5, 11.5, and 12.5).

The lattice parameter was calculated using the formula (6) and found to be $a = 4.2692 \text{ \AA}$, which are almost in agreement with the standard data from JCPDS card No. 01-078-2076 ($a = b = c = 4.2612 \text{ \AA}$) [36].

$$\frac{1}{d^2} = \frac{h^2}{a^2} + \frac{k^2}{b^2} + \frac{l^2}{c^2} \quad (1)$$

The crystallite size of the film was calculated from the intense peak of (111) plan by using Scherer's formula Eq (7) [37,38]:

$$D = \frac{k\lambda}{\beta \cos(\theta)} \quad (2)$$

where, λ is the used wavelength (1.5406 \AA); β is the angular line width at half maximum intensity (FWHM) of the diffraction peaks (in radians); θ is the Bragg's angle, and k is the constant, which is equal to 0.94. To have more information on the measure of imperfections in the films, the dislocation density (δ) was determined using the formula (8) [37,38].

$$\delta = \frac{1}{D^2} \quad (3)$$

The strain (ϵ) was calculated using the equation (9) [37,38].

$$\varepsilon = \frac{\beta \cos(\theta)}{4} \tag{4}$$

The variation of structural parameters is shown in table (1). It is observed that when the pH increase, the Crystallite size increase. Conversely, the dislocation density and microstrain decrease with the increase of pH.

Table 1. Structural parameters obtained from the (111) plane for the synthesized Cu₂O thin films.

pH of deposition	Miller indices	Observation diffraction angle (°)	FWHM (β) (°)	Crystallite size (D) (nm)	Dislocation density (δ) (x10 ⁻³ nm ⁻²)	Microstrain (ε) (x10 ⁻³)
9.5	1 1 1	36.24	0.635	2.27	194	133
10.5		36.37	0.624	2.31	187	131
11.5		36.31	0.604	2.40	173	127

3.2. Raman spectroscopy analysis.

The Raman technique was used with a 633 nm excitation wavelength. As copper (II) oxide, Cu₂O is a material that occurs in a cubic Pn-3m phase [36]. There are 6 atoms in the unit cell of Cu₂O, and therefore 18 phonon branches.

$$\Gamma = A_{2u} \oplus E_u \oplus 3T_{1u} \oplus T_{2u} \oplus T_{2g}$$

where A, E, and T symmetry are one-, two-, and three-fold degenerated, respectively. In Figure 2, we can resolve sept broad bands in our Raman Spectra. According to the results obtained by Raman spectrometry, two active modes E_u and T_{1u}, were observed, and the absence of A_{2u} and T_{2g} modes. Figure 2 shows the Raman spectrum of Cu₂O thin films within 100 – 700 cm⁻¹. The peaks located at 108 cm⁻¹ (E_u), 148 cm⁻¹ (T_{1u}), 214 cm⁻¹ (2E_u), 297 cm⁻¹, 413 cm⁻¹ (2E_u), 495 cm⁻¹ (2E_u), and 647 cm⁻¹ (T_{1u}) are characteristic of the cubic Cu₂O thin films, which is in good agreement well with other literature [39].

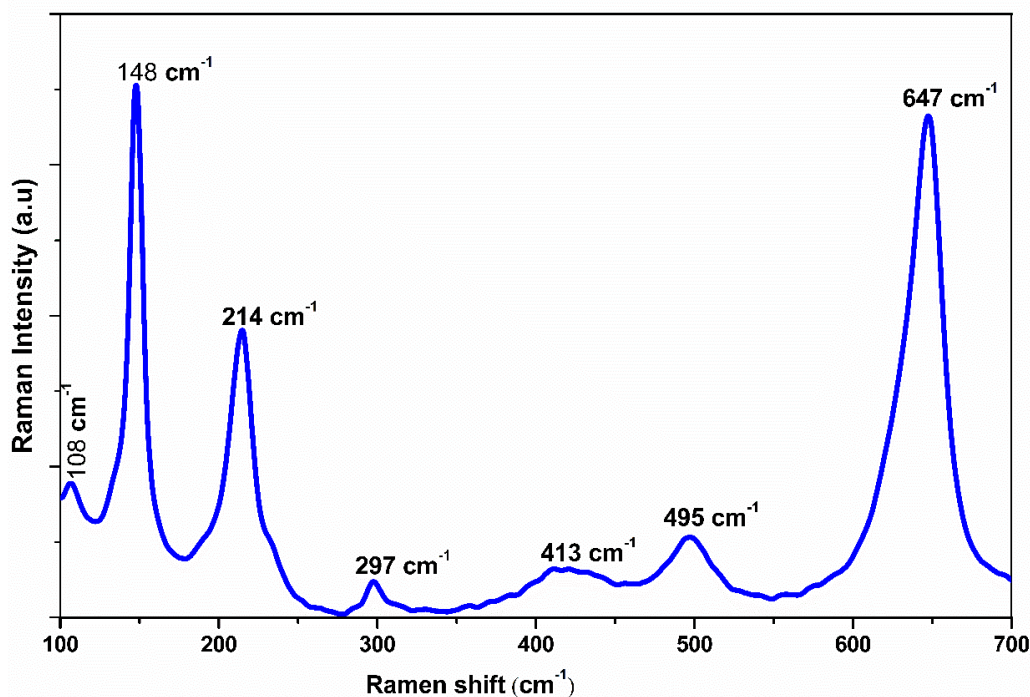


Figure 2. Raman spectra of electrodeposited Cu₂O at PH=10.5 and applied potentials (-0.2V; -0.4V).

3.3. Morphological properties.

Figure 3 (a-c) shows the SEM image of Cu₂O thin films electrodeposited at different pH (9.5, 10.5, and 11.5). The Cu₂O detected by SEM presents a uniform surface coverage with

good crystalline quality confirming XRD analysis and showing numerous well-distributed pyramid-like nanostructures (Figure 2). The sample prepared at pH=9.5 and Cu₂O shows a homogeneous nanostructure. When the pH increases to 10.5, the nanostructure becomes apparent with uniform pyramid distribution, as shown in Figure 3(b). Finally, for pH=11.5, the nano-grains were none uniformly distributed on the smooth surface, with variable size, and we observed the presence of some void.

Furthermore, the elemental mapping analyses (Figure 3 d-e) confirm the existence of Cu and O and indicate that the distributions of Cu and O are uniform, with the absence of the pinholes, confirming the homogeneous and uniform depositing Cu₂O thin films. The EDX (Figure 4) confirms the copper and oxygen atoms that make up our thin film. However, the quotient Cu/O is equal to 2.1 (55.61 at. % Cu and 45.39 at. % O) (Figure 4) against the ideal value of 2 for pure Cu₂O, which may be due to the copper substrate.

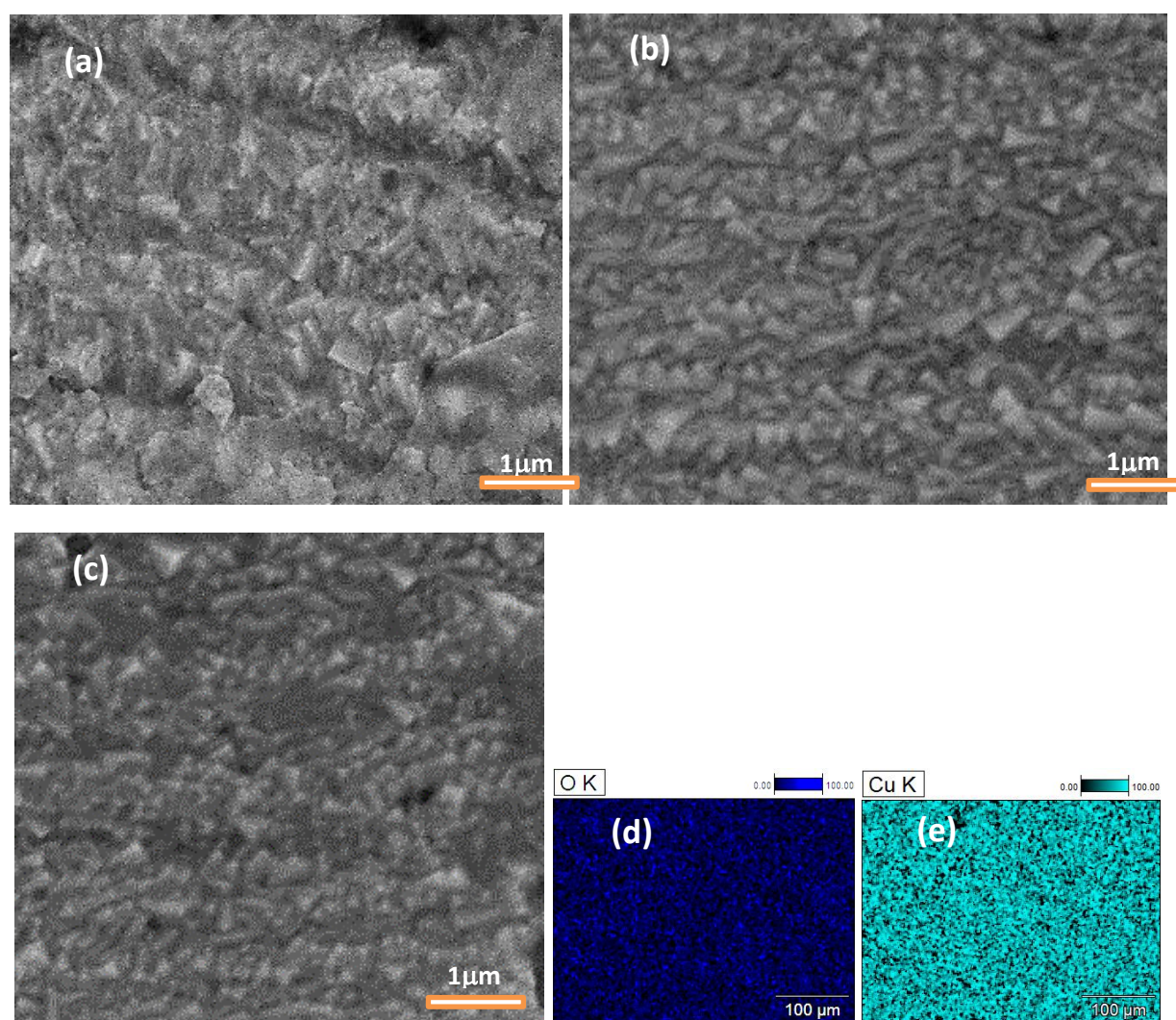


Figure 3. SEM micrographs of Cu₂O thin films electrodeposited at different pH (a)9.5; (b) 10.5; (c) 11.5. (d, e): EDX-mapping of Cu and O at pH= 10.5.

3.4. Optical properties.

The optical absorption properties of Cu₂O thin films electrodeposited onto copper substrates are determined from UV-Vis transmittance spectra in the range 400 – 650nm and are shown in Figure 5. (A). Firstly, all the films indicated a better absorption in the solar spectrum's 400-500 nm spectral region. The absorbance spectra show a high absorbance for the <https://biointerfaceresearch.com/>

Cu₂O thin films at wavelengths below 500 nm with sharp optical absorption transitions at 457 nm. This absorption is due to the inter-band electron transition between the valence and conduction bands in the Cu₂O thin film [40, 41].

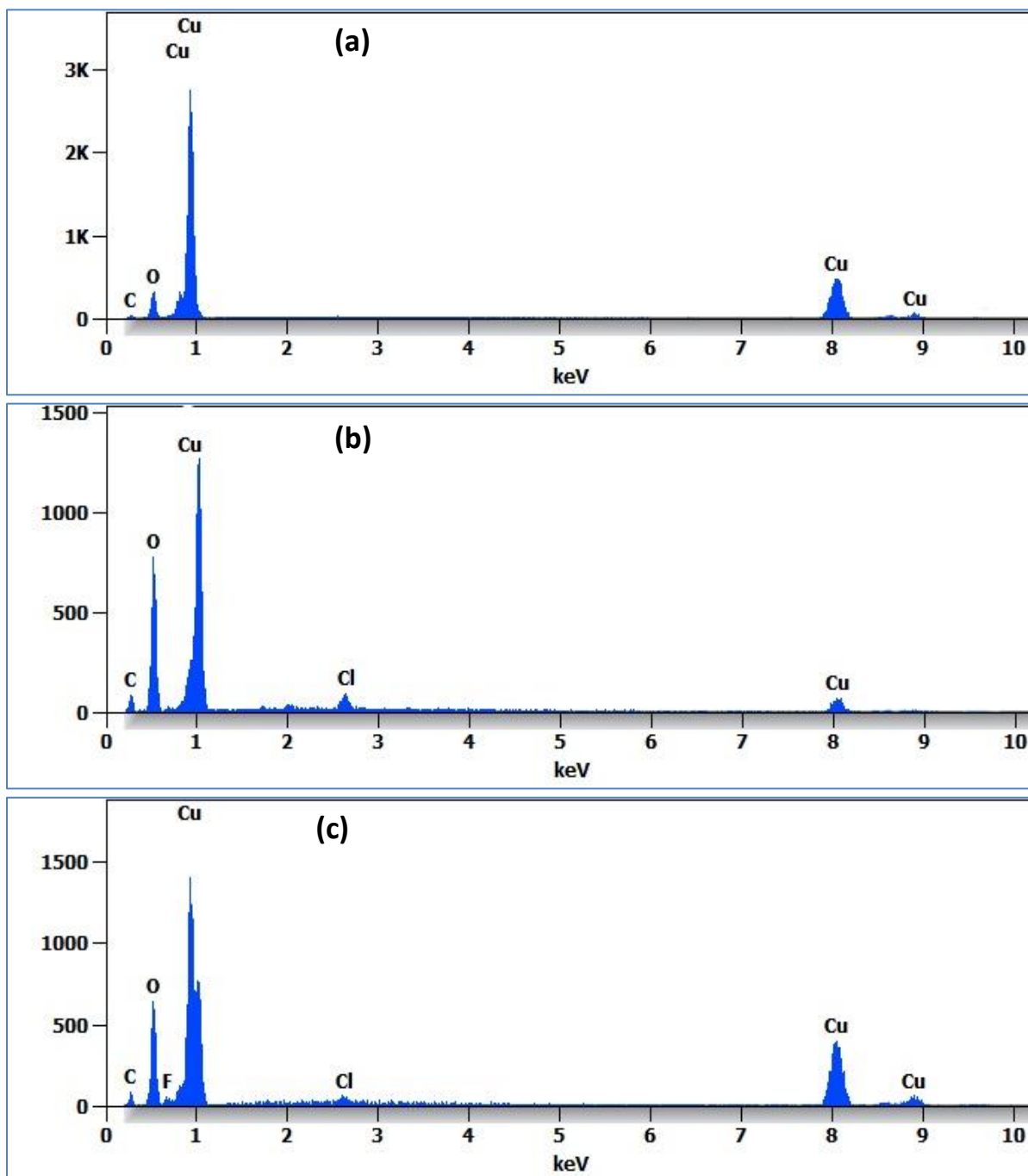


Figure 4. EDX spectrum of Cu₂O thin films electrodeposited at different pH (a) 9.5; (b) 10.5; (c) 11.5.

Figure 5 shows that the sample deposited at pH=10.6 exhibits the highest optical absorbance at most wavelengths, especially in the wavelength range below 500 nm, and the light absorbance in Cu₂O thin films notably reduces increasing the deposition time.

The bandgap values are determined by applying the Tauc's relationship (Eq.10) [42,43] and were obtained from extrapolating the linear region of the plot $(\alpha \cdot hv)^2$ versus energy hv (Figure 6), which indicates the existence of direct transitions.

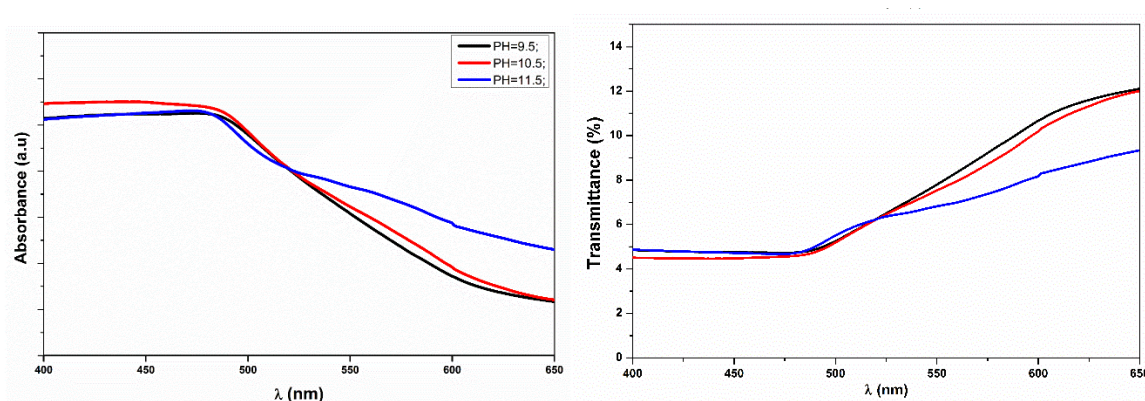


Figure 5. Absorbance and transmittance spectra of Cu₂O thin films deposited on copper substrates at different pH.

$$(\alpha h\nu)^2 = A(h\nu - E_g) \tag{5}$$

where, $h\nu$ is the photon energy, A is a constant characteristic of the semiconductor, and α is the absorption coefficient. The used thickness of the film to calculate α is about 800nm.

The values of the bandgap E_g of Cu₂O thin films deposited at pH= 9.5, 10.5, and 11.5 are found to be 1.80 eV, respectively, which are well suited for solar cell application and near the other reported value [44]. The use of copper substrate has permitted the reduction of band gap value (1.8eV) compared to other reports. The band gaps (E_g) values are not affected by the variation of pH value.

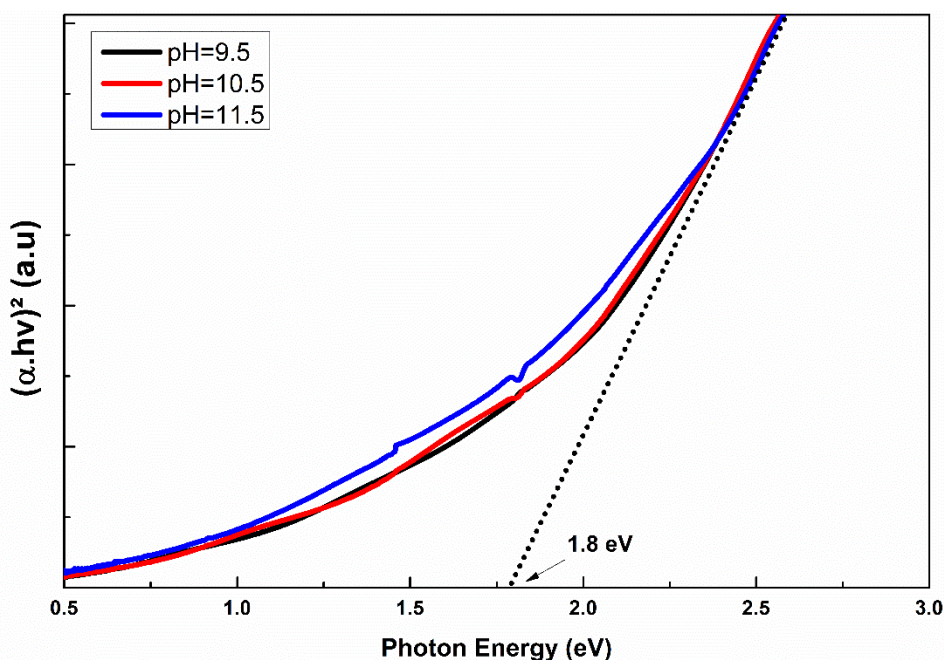


Figure 6. The $(\alpha \cdot hv)^2$ versus $h\nu$ plot for Cu₂O thin-films deposited at pH= 9.5, 10.5 and 11.5.

4. Conclusions

The Cu₂O thin films were successfully deposited by the linear sweep voltammetry (LSV) method at low duration on the copper substrate using the precursor copper sulfate and citric acid as a stabilizing agent. Summing up the resultants, it can be concluded that the crystallographic parameters, stoichiometry, morphological, and Raman analysis were showed the presence of cubic Cu₂O and have a preferred orientation along (111) planes due to the

copper substrate. Micrograph indicates the small pyramid nanostructure, homogeneous, dense, and adherent layers. The use of copper substrate has permitted the reduction of band gap value (1.8eV) compared to other reports and is not affected by the pH variation. Moreover, the absorption coefficient could reach the order of 10^5 cm^{-1} in the visible. This makes Cu_2O a promising material for solar cell application by the linear sweep voltammetry technique, and it can benefit from high photosensitivity and low-cost production.

Funding

This research received no external funding.

Acknowledgments

We thank all colleagues.

Conflicts of Interest

The authors declare no conflict of interest.

References

1. Chatterjee, S.; Sudip, K-S.; Amlan, J-P. Formation of all-oxide solar cells in atmospheric condition based on Cu_2O thin-films grown through SILAR technique. *Solar Energy Materials & Solar Cells*. **2016**, *147*, 17-26, <https://doi.org/10.1016/j.solmat.2015.11.045>.
2. Beraich, M.; Shaili, H.; Benhsina, E.; Hafidi, Z.; El hat, A.; Taibi, M.; Bentiss, F.; Guenbour, A.; Bellaouchou, A.; Mansouri, S.; Mzerd, A.; Zarrouk, A.; Fahoume, M. Structural, electronic and optical properties of a tetragonal-stannite $\text{Cu}_2\text{CoGeS}_4$ thin film synthesized by a low-cost spray method: *Experimental and theoretical study*, *Ceram. Int.* **2020**, *46*, 23127–23133, <https://doi.org/10.1016/j.ceramint.2020.06.090>.
3. Beraich, M.; Shaili, H.; Benhsina, E.; Hafidi, Z.; Mansouri, S.; Taibi, M.; Bentiss, F.; Guenbour, A.; Bellaouchou, A.; Mzerd, A.; Zarrouk, A.; Fahoume, M. Preparation and characterization of $\text{Cu}_2\text{FeGeS}_4$ thin-film synthesized via spray ultrasonic method – DFT study. *Mater Lett.* **2020**, *275*, 2–5, <https://doi.org/10.1016/j.matlet.2020.128070>.
4. Zoofakar, A-S.; Rani Abdul, R.; Morfa, A-J.; O'Mullane, A-P.; Kalantar-Zadeh, K. Nanostructured copper oxide semiconductors: a perspective on materials, synthesis methods and applications. *J. Mater. Chem. C*. **2014**, *2*, 5247–5270, <https://doi.org/10.1039/C4TC00345D>.
5. Xue, J.; Shen, Q.; Liang, W.; Liu, X.; Bian, L.; Xu, B. Preparation and formation mechanism of smooth and uniform Cu_2O thin films by electrodeposition method. *Surf. Coat. Technol* **2013**, *216*, 166–171, <https://doi.org/10.1016/j.surfcoat.2012.11.051>
6. Akter, J.; Sapkota, K-P.; Hanif, M-A.; Islam, M-A.; Abbas, H-G.; Hahn, J-R. Kinetically controlled selective synthesis of Cu_2O and CuO nanoparticles toward enhanced degradation of methylene blue using ultraviolet and sun light. *Mater, Sci, Semicond, Process* **2021**, *123*, 105570, <https://doi.org/10.1016/j.msssp.2020.105570>.
7. Zhou, X.; Yin, A.; Sheng, J.; Wang, J.; Chen, H.; Fang, Y.; Zhang, K. In situ deposition of nano Cu_2O on electrospun chitosan nanofibrous scaffolds and their antimicrobial properties. *Int, J, Biol, Macromol.* **2021**, *191*, 600-607, <https://doi.org/10.1016/j.ijbiomac.2021.09.121>.
8. Cui, J.; Gibson, U-J. A simple two-step electrodeposition of $\text{Cu}_2\text{O}/\text{ZnO}$ nanopillar solar cells. *J.Phys.Chem, C.* **2010**, *114*, 6005-6011, <https://doi.org/10.1021/jp1004314>.
9. Wang, L-C.; De Tacconi, N-R. ; Chenthamarakshan, C R. et al. Electrodeposition copper oxide films: effect of bath pH on grain orientation and orientation-dependant interfacial behavior. *Thin Solid Films.* **2007**, *515*, 3090, <https://doi.org/10.1016/j.tsf.2006.08.041>.
10. Bayat, F.; Sheibani, S. Enhancement of photocatalytic activity of $\text{CuO}-\text{Cu}_2\text{O}$ heterostructures through the controlled content of Cu_2O . *Materials Research Bulletin* **2022**, *145*, 111561, <https://doi.org/10.1016/j.materresbull.2021.111561>.
11. Sahu, K.; Bisht, A.; Pandey, A.; Dutta, A.; Khan, S-A.; Singhal, R.; Som, T.; Mohapatra, S. RF magnetron sputtered $\text{Ag}-\text{Cu}_2\text{O}-\text{CuO}$ nanocomposite thin films with highly enhanced photocatalytic and catalytic performance. *Appl. Surf. Sci.* **2020**, *517*, 146169, <https://doi.org/10.1016/j.apsusc.2020.146169>.

12. Wang, P.; Wu, H.; Tang, Y et al. Electrodeposited Cu₂O as photoelectrodes with controllable conductivity type for solar energy conversion. *J Phys Chem C*. **2015**, *119*, 26275–2628, <https://doi.org/10.1021/acs.jpcc.5b07276>.
13. Trenczek-Zajac, A.; Banas-Gac, J.; Radecka, M. TiO₂@Cu₂O n-n Type Heterostructures for Photochemistry. *Materials* **2021**, *14*, 3725, <https://doi.org/10.3390/ma14133725>.
14. Thalluri, S.M.; Bai, L.; Lv, C.; Huang, Z.; Hu, X.; Liu, L. Strategies for Semiconductor/Electrocatalyst Coupling toward Solar Driven Water Splitting. *Adv. Sci.* **2020**, *7*, <https://doi.org/10.1002/advs.201902102>.
15. Bai, Z-M.; Zhang, Y-H.; Huang, Z-A.; Gao, Y-K.; Liu, J. Performance optimization of self-powered visible photodetectors based on Cu₂O/electrolyte heterojunctions. *Chinese Phys B*. **2020**, *29*, 128202, <https://doi.org/10.1088/1674-1056/abab7b>.
16. Chen, X.; Parker, D.; Du, M-H.; David, J. Singh Potential thermoelectric performance of hole-doped Cu₂O. *New J. Phys.* **2013**, *15*, 043029, <https://doi.org/10.1088/1367-2630/15/4/043029>.
17. Hsueh H-T.; Chang S-J.; Hung F-Y.; Weng, W-Y.; Hsu, C-L.; Hsueh, T-J.; Tsai, T-Y.; Dai, B-T. Fabrication of coaxial p-Cu₂O/n-ZnO nanowire photodiodes. *Superlattices and Microstructures* **2011**, *49*, 572, <https://doi.org/10.1016/j.spmi.2011.03.011>.
18. Wick, R.; Tilley, S-D. Photovoltaic and photoelectrochemical solar energy conversion with Cu₂O. *J Phys Chem C*. **2015**, *119*, 26243– 26257, <https://doi.org/10.1021/acs.jpcc.5b08397>.
19. Poizot, P.; Laruelle, S.; Grugeon, S.; Dupont, L.; Tarascon J-M. Nano-sized transition-metal oxides as negative-electrode materials for lithium-ion batteries. *Nature* **2000**, *407*, 407-496, <https://doi.org/10.1038/35035045>.
20. Yan, D.; Li, S.; Hu M.; Liu, S.; Zhu, Y.; Cao, M. Electrochemical synthesis and the gas sensing properties of the Cu₂O nanofilms/porous silicon hybrid structure. *Sensors and Actuators B*. **2016**, *223*, 626, <https://doi.org/10.1016/j.snb.2015.09.080>.
21. Niu, L.; Kang, Z.; Spray deposition process to fabricate Cu₂O superhydrophobic surfaces on brass mesh for efficient oil-water separation, *Mater. Lett.* **2018**, *210*, 97–100, <https://doi.org/10.1016/j.matlet.2017.08.105>.
22. McShane, C-M.; Choi, K-S. Photocurrent enhancement of ntype Cu₂O electrodes achieved by controlling dendritic branching growth. *J am Chem Soc.* **2009**, *131*, 2561–2569, <https://doi.org/10.1021/ja806370s>.
23. Jayathilaka, C.; Kumara, L.S.R.; Ohara, K.; Song, C.; Kohara, S.; Sakata, O.; Siripala, W.; Jayanetti, S. Enhancement of Solar Cell Performance of Electrodeposited Ti/n-Cu₂O/p-Cu₂O/Au Homojunction Solar Cells by Interface and Surface Modification. *Crystals* **2020**, *10*, 609, <https://doi.org/10.3390/cryst10070609>.
24. Rosas-Laverde, N.M.; Pruna, A.I.; Cembrero, J.; Busquets-Mataix, D. Electrodeposition of ZnO/Cu₂O Heterojunctions on Ni-Mo-P Electroless Coating. *Coatings* **2020**, *10*, 935, <https://doi.org/10.3390/coatings10100935>.
25. Sakellis, E.; Markopoulos, A.; Tzouvelekis, C.; Chatzigeorgiou, M.; Travlos, A.; Boukos, N. Low-Cost Electrodeposition of Size-Tunable Single-Crystal ZnO Nanorods. *Fibers* **2021**, *9*, 38, <https://doi.org/10.3390/fib9060038>.
26. Hssi, A. A.; Atourki; L.; Labchir, N.; Abouabassi, K.; Ouafi, M.; Mouhib, H.; Ihlal, A.; Elfanaoui, A.; Benmokhtar, S.; Bouabid, K. Structural and optical properties of electrodeposited Cu₂O thin films. *Materials Today: Proceedings* **2020**, *22*, 89-92, <https://doi.org/10.1016/j.matpr.2019.08.100>.
27. Alsultany, F-H. One-step chemical bath deposition of Cu₂O flowers grown on ITO seed layer coated glass substrate. *IOP Conf. Ser.: Mater. Sci. Eng.* **2019**, *557*, 012081, <https://doi.org/10.1088/1757-899X/557/1/012081>.
28. Al-Kuhaili, M F. Characterization of copper oxide thin films deposited by the thermal evaporation of cuprous oxide (Cu₂O). *Vacuum*. **2008**, *82*, 623, <https://doi.org/10.1016/j.vacuum.2007.10.004>.
29. Delatorre, R-G.; Munford, M-L.; Zandonay, R.; Zoldan, V-C.; Pasa, A-A. p-Type metal-base transistor. *Appl Phys Lett*. **2006**, *88*, 233504, <https://doi.org/10.1063/1.2202825>.
30. Suzuki, S.; Miyata, T.; Minami T. p -type semiconducting Cu₂O–CoO thin films prepared by magnetron sputtering. *J Vac Sci Technol A Vacuum, Surfaces, Film.* **2003**, *21*, 1336–1341, <https://doi.org/10.1116/1.1580491>.
31. Daoudi, O.; Qachaou, Y.; Raidou, A.; Nouneh, K.; Lharch, M.; Fahoume, M. Study of the physical properties of CuO thin films grown by modified SILAR method for solar cells applications. *Superlattices Microstruct.* **2019**, *127*, 93–99, <https://doi.org/10.1016/j.spmi.2018.03.006>.
32. Beraich, M.; Taibi, M.; Guenbour, A.; Zarrouk, A.; Bellaouchou, A.; Fahoume, M. Synthesis of Tetragonal Cu₂NiSnS₄ Thin Film via Low-Cost Electrodeposition Method: Effect of Ni²⁺ Molarity. *J. Electron. Mater.* **2020**, *49*, 728–735, <https://doi.org/10.1007/s11664-019-07707-4>.
33. Rahal, H.; Kihal, R.; Affoune, A-M.; Rahal, S. Electrodeposition and characterization of Cu₂O thin films using sodium thiosulfate as an additive for photovoltaic solar cells. *Chinese J. Chem. Eng.* **2018**, *26*, 421–427, <https://doi.org/10.1016/j.cjche.2017.06.023>.
34. Saha, S.; Johnson, M.; Altayaran, F.; Wang, Y.; Wang, D.; Zhang, Q. Electrodeposition Fabrication of Chalcogenide Thin Films for Photovoltaic Applications. *Electrochem* **2020**, *1*, 286-321, <https://doi.org/10.3390/electrochem1030019>.

35. Oliveri, R.L.; Patella, B.; Di Pisa, F.; Mangione, A.; Aiello, G.; Inguanta, R. Fabrication of CZTSe/CIGS Nanowire Arrays by One-Step Electrodeposition for Solar-Cell Application. *Materials* **2021**, *14*, 2778, <https://doi.org/10.3390/ma14112778>.
36. Tian, X.; Wen, J.; Chen, Z.; Liu, X.; Peng, H.; Ji, C.; Li, J.; Peng, Y.; He, H. One-pot green hydrothermal synthesis and visible-light photocatalytic properties of Cu₂O/Cu hybrid composites using egg albumin as structure modifier. *Solid State Sci.* **2019**, *93*, 70–78, <https://doi.org/10.1016/j.solidstatesciences.2019.04.013>.
37. Shaili, H.; Salmani, E.; Beraich, M.; Elhat, A.; Rouchdi, M.; Taibi, M.; Ez-zahraouy, H.; Hassanain, N.; Mzerd, A. optical , electronic and electrical properties of nanostructured 2H-CuFeO₂ delafossite thin films. *RSC Adv.* **2021**, *11*, 25686–25694, <https://doi.org/10.1039/D1RA03734J>.
38. Shaili, H.; Mehdi Salmani, E.; Essajai, R.; Beraich, M.; Battal, W.; Ouafi, M.; Elhat, A.; Rouchdi, M.; Ez-Zahraouy, H.; Hassanain, N.; Mzerd, A. Structural, electronic and optical properties of Cu-doped ZnS thin films deposited by the ultrasonic spray method- DFT study. *Opt. Quantum Electron.* **2021**, *53*, 1–15, <https://doi.org/10.1007/s11082-021-02934-8>.
39. Sander, T.; Reindl, C-T.; Klar, P-J. Breaking of Raman selection rules in Cu₂O by intrinsic point defects. *J. Br. Stud.* **2014**, *1633*, 81–86, <https://doi.org/10.1557/opl.2014.47>.
40. Yin, M.; Wu, C-K.; Lou, Y.; Burda, C.; Koberstein, J-T.; Zhu, Y.; O'Brien, S. Copper oxide nanocrystals. *J. Am. Chem. Soc.* **2005**, *127*, 9506–9511, <https://doi.org/10.1021/ja050006u>.
41. Messaoudi, O.; Ben assaker, I.; Gannouni, M.; Souissi, A.; Makhoulf, H.; Bardaoui, A.; Chtourou, R. Structural, morphological and electrical characteristics of electrodeposited Cu₂O: Effect of deposition time, *Appl. Surf. Sci.* **2016**, *366*, 383–388, <https://doi.org/10.1016/j.apsusc.2016.01.035>.
42. Beraich, M.; Taibi, M.; Guenbour, A.; Zarrouk, A.; Boudalia, M.; Bellaouchou, A.; Tabyaoui, M.; Sekkat, Z.; Fahoume, M. Synthesis and characterization of Cu₂CoSnS₄ thin film via electrodeposition technique for solar cells. *J. Mater. Sci. Mater. Electron.* **2019**, *30*, 12487–12492, <https://doi.org/10.1016/j.ijleo.2019.162996>.
43. Rahal, H.; Kihal, R.; Affoune, A.M.; Rahal, S. Effect of Solution pH on Properties of Cuprous Oxide Thin Films Prepared by Electrodeposition from a New Bath. *J. Electron. Mater.* **2020**, *49*, 4385–4391, <https://doi.org/10.1007/s11664-020-08093-y>.
44. Kim, G.; Oh, H-B.; Ryu, H.; Lee, W-J. The study of post annealing effect on Cu₂O thin-films by electrochemical deposition for photoelectrochemical applications. *J. Alloys Compd.* **2014**, *612*, 74–79, <https://doi.org/10.1016/j.jallcom.2014.05.158>.